Fingolimod sensitizes *EGFR* wild-type non-small cell lung cancer cells to lapatinib or sorafenib and induces cell cycle arrest

KOHKI OTA[1], TAKASHI OKUMA[1], ALBERTO DE LORENZO[1,2], AYUKA YOKOTA[1], HIROTSUGU HINO[1], HIROMI KAZAMA[1], SHOTA MORIYA[1], NAOHARU TAKANO[1], MASAKI HIRAMOTO[1] and KEISUKE MIYAZAWA[1]

[1]Department of Biochemistry, Tokyo Medical University, Tokyo 160-8402, Japan; [2]International Medical School, University of Milan, I-20122 Milan, Italy

Received August 29, 2018; Accepted April 2, 2019

DOI: 10.3892/or.2019.7140

Abstract. Epidermal growth factor receptor (EGFR) is a receptor tyrosine kinase and mutations in this gene are major drivers of lung cancer development. EGFR tyrosine kinase inhibitors (TKIs) are standard first-line therapies for patients with advanced non-small cell lung cancer (NSCLC) with activating *EGFR* mutations, but are not effective in patients with wild-type *EGFR*. In the present study, the cytotoxic effects of various TKIs against EGFR were investigated in wild-type NSCLC cells as single treatments or in combination with Fingolimod (FTY720), which has been approved for treating multiple sclerosis and has cytotoxic effects against several tumor cell lines. It was found that the combined treatment with TKIs lapatinib (Lap) or sorafenib (Sor) and FTY720 synergistically suppressed the viability of the NSCLC cell lines A549 and H596. Additionally, FTY720 inhibited lysosomal acidification and suppressed autophagy flux. Immunoblotting and reverse transcription-quantitative polymerase chain reaction showed that FTY720 combined with Lap or Sor, enhanced endoplasmic reticulum (ER) stress loading and cell cycle arrest in A549 cells. The enhancement of ER stress loading and cell cycle arrest induced by combined treatment with Lap or Sor and FTY720, which was associated with the cytotoxicity induced by the combination of these drugs. These findings suggested that FTY720 improved TKI therapy in NSCLC patients with wild-type *EGFR*, by sensitizing NSCLC cells to TKIs.

Correspondence to: Dr Masaki Hiramoto, Department of Biochemistry, Tokyo Medical University, 6-1-1 Shinjuku, Shinjuku-ku, Tokyo 160-8402, Japan
E-mail: hiramoto@tokyo-med.ac.jp

Abbreviations: EGFR, epidermal growth factor receptor; TKIs, tyrosine kinase inhibitors; NSCLC, non-small cell lung cancer; ER, endoplasmic reticulum; UPR, unfolded protein response; Sor, sorafenib; Gef, gefitinib; Erl, erlotinib; Lap, lapatinib; Ima, imatinib; Tg, thapsigargin; Tm, tunicamycin; BafA1, bafilomycin A1; FTY720-P, FTY720 (S)-phosphate; Z-VAD, Z-VAD-FMK; Nec-1, Necrostatin-1; DMSO, dimethyl sulfoxide; SDS, sodium dodecyl sulfate; siRNA, small interfering RNA; ANOVA, analysis of variance

Key words: non-small cell lung cancer, epidermal growth factor receptor, Fingolimod, tyrosine kinase inhibitors, endoplasmic recticulum stress loading, cell cycle arrest

Introduction

Lung cancer is the second most common cancer and the leading cause of cancer-associated mortality worldwide. The vast majority of lung cancer cases are non-small cell lung cancer (NSCLC) (1,2). Epidermal growth factor receptor (EGFR) is a receptor tyrosine kinase that belongs to the ErbB family and mutations in this gene are a major driver of lung cancer (3-9). Mutations in the tyrosine kinase region of EGFR involving the L858R substitution or small internal deletions of exon 19, lead to constitutive activation of EGFR (10). EGFR tyrosine kinase inhibitors (TKIs) such as gefitinib (Gef) and erlotinib (Erl) inhibit the phosphorylation of EGFR, preventing the subsequent activation of the downstream signaling networks, which would lead to cancer cell proliferation and survival (11). EGFR TKIs are standard first-line therapies for patients with advanced NSCLC with activating *EGFR* mutations, whereas they show low efficacy in patients with wild-type *EGFR* (12-16). Therefore, additional therapeutic strategies are urgently necessary for NSCLC patients with wild-type *EGFR*.

Since the first TKI drug imatinib (Ima) was approved for the treatment of chronic myeloid leukemia in 2001, more than 20 TKIs have been approved by the FDA. Lapatinib (Lap), which is used to treat advanced or metastatic breast cancer, is a reversible dual inhibitor of EGFR and ERBB2. The response to Lap is strongly associated with ERBB2 overexpression, which inhibits the phosphorylation of ERBB2 and its subsequent signaling molecules (17). Sorafenib (Sor) is the first anti-tumor drug targeting RAF kinase and VEGFR, that is approved for treating renal cell and hepatocellular carcinomas. This agent can directly inhibit tumor cell proliferation by blocking the RAF/MEK/ERK signaling pathway and by inhibiting VEGFR-mediated angiogenesis (18).

Fingolimod (FTY720), a sphingosine analog, was recently shown to be highly effective for treating relapsing-remitting

multiple sclerosis (19). In addition to its immunomodulatory effects, FTY720 showed preclinical antitumor efficacy in several cancer models (20-23). In most cases, the anticancer mechanism of FTY720 involves inhibition of the proto-oncogene sphingosine kinase 1; however, the anticancer properties of FTY720 may be attributable to its effects on several other molecular targets (24,25). Furthermore, FTY720 was reported to modulate autophagy; a number of studies have reported the induction of autophagy by FTY720 (26-29), while others have reported autophagy suppression (30-33). Autophagy exhibits complex, context-dependent properties in cancer, and interventions that stimulate or inhibit autophagy have been proposed as potential anti-cancer therapies (34).

Drug repositioning, which is the discovery of new medical indications for existing drugs that are different from their original indications, is an increasingly attractive mode of therapeutic discovery (35-37). We previously reported that macrolide antibiotics, such as clarithromycin and azithromycin, block autophagy flux and that the combination of Gef with macrolide antibiotics enhances the cytotoxic effect in NSCLC cells via endoplasmic reticulum (ER)-stress loading (38). Under remediable levels of ER stress, the homeostatic unfolded protein response (UPR) outputs activate transcriptional and translational changes that promote cellular adaptation (39-41). Contrary to its pro-survival roles, prolonged UPR activation caused by severe or unresolved ER stress leads to cell death (39-41). In the present study, in order to discover more effective combinations of the existing drugs, the cytotoxic effects of various TKIs against *EGFR* wild-type NSCLC cells were investigated, using TKIs in single or combination treatments with FTY720 as the repurposed candidate drug.

Materials and methods

Reagents. Gef, Erl, Lap, Sor and FTY720 were purchased from Cayman Chemical Company (Ann Arbor, MI, USA). Ima was obtained from Tokyo Chemical Industry Co., Ltd. (Tokyo, Japan). These drugs were dissolved in dimethyl sulfoxide (DMSO) at a concentration of 20 mM as a stock solution. FTY720 (S)-phosphate (FTY720-P) was also purchased from Cayman Chemical Company and dissolved in DMSO at a concentration of 0.5 mM as a stock solution. Thapsigargin (Tg) and bafilomycin A1 (BafA1) were purchased from Wako Pure Chemical Industries, Ltd. (Osaka, Japan). Tunicamycin (Tm) was purchased from Nacalai Tesque, Inc. (Kyoto, Japan). Z-VAD-FMK (Z-VAD), a pan-caspase inhibitor, was purchased from Peptide Institute, Inc. (Osaka, Japan). Necrostatin-1 (Nec-1), a specific inhibitor of receptor-interacting serine/threonine-protein kinase 1 (RIPK1), was purchased from Enzo Life Sciences, Inc. (Farmingdale, NY, USA). Azithromycin was purchased from Tokyo Chemical Industry Co., Ltd. These reagents: Tg, BafA1, Tm, Z-VAD, Nec-1 and azithromycin were also dissolved in DMSO as a stock solution.

Cell lines. Human NSCLC cell lines A549, H596, and H226, as well as the ERBB2-positive breast cancer cell line BT474 were purchased from American Type Culture Collection (Manassas, VA, USA). These cell lines were cultured in RPMI-1640 medium (Sigma-Aldrich; Merck KGaA, Darmstadt, Germany), supplemented with 10% heat inactivated fetal bovine serum (Biosera, Nuaillé, France) at 37˚C in a 5% CO_2 atmosphere. Stable A549/GFP-LC3-RFP-LC3ΔG cell lines were generated as follows: A549 cells ($2x10^6$ cells/100 mm dish) were transfected with the plasmid DNA (GFP-LC3-RFP-LC3ΔG plasmid, 10 μg) using Lipofectamine® 3000 (Thermo Fisher Scientific, Inc., Waltham, MA, USA) according to the manufacturer's instructions. The GFP-LC3-RFP-LC3ΔG plasmid used in the present study was a kind gift from Dr N. Mizushima (University of Tokyo, Tokyo, Japan). After selecting transfected cells using puromycin (2 μg/ml), single clones of the cells were isolated, and GFP-LC3 and RFP-LC3ΔG expression was confirmed by immunoblotting using specific antibodies against green fluorescent protein (GFP), red fluorescent protein (RFP), and microtubule associated proteins 1A/1B light chain 3B (MAP1LC3B).

Cell viability assay. The number of viable cells was assessed by the CellTiter Blue cell viability assay kit (Promega Corporation, Madison, WI, USA) according to the manufacturer's instructions. Briefly, cells were incubated with the CellTiter Blue reagent for 2 h at 37˚C in 5% CO_2 atmosphere. Fluorescence (560 nm for excitation and 590 nm for emission) was measured using the POWERSCAN HT 96-well plate reader (BioTek Instruments, Inc., Winooski, VT, USA). In order to determine IC_{50} (half-maximal inhibitory concentration) values, A549 cells treated with different concentrations of TKIs or FTY720 were tested for cell viability at 48 h after the treatments. Dose response curves were fitted and IC_{50} values were analyzed using the four-parameter logistic regression analysis by means of ImageJ software (version 1.52a).

Immunoblotting. Total cellular proteins were extracted using radioimmunoprecipitation assay lysis buffer containing 50 mM Tris-HCl (pH 8.0), 150 mM NaCl, 1.0% Nonidet P-40, 0.5% sodium deoxycholate, 0.1% sodium dodecyl sulfate (SDS), and a protease inhibitor cocktail (Nacalai Tesque, Inc.). Each sample was sonicated for 20 pulses (0.5 sec on/off) to disrupt the aggregated proteins, using a Branson 450D Sonifier (Emerson, Danbury, CT, USA). Protein concentrations were measured using a Bicinchoninic Acid Protein Assay kit (Pierce; Thermo Fisher Scientific, Inc.) according to the manufacturer's instructions. Equal amounts of proteins were resolved by SDS-PAGE (5-20% gradient gel) and transferred onto Immobilon-P membranes (EMD Millipore, Billerica, MA, USA). The membranes were then blocked with 5% non-fat milk for 1 h at room temperature and probed with the following primary antibodies at 4˚C overnight: Anti-MAP1LC3B (cat. no. NB600-1384; 1:4,000 dilution; Novus Biologicals, Inc. Littleton, CO, USA). Anti-sequestosome (SQSTM1; cat. no. sc-28359; 1:1,000 dilution), anti-GAPDH (cat. no. sc-32233; 1:2,000 dilution), anti-heat shock protein family A member 5 (HSPA5; cat. no. sc-13968; 1:1,000 dilution), anti-β-actin (cat. no. sc-47778; 1:2,000 dilution), anti-EGFR (cat. no. sc-03; 1:1,000 dilution), and anti-phosphorylated (p)-EGFR (Tyr1173; cat. no. sc-101668, 1:1,000 dilution) from Santa Cruz Biotechnology, Inc. (Santa Cruz, CA, USA); anti-cyclin D (CCND)1 (cat. no. 2978, 1:1,000 dilution), anti-CCND3 (cat. no. 2936, 1:1,000 dilution), anti-cyclin-dependent kinase (CDK)4 (cat. no. 12790, 1:1,000 dilution), anti-CDK6 (cat. no. 3136, 1:1,000 dilution),

anti-DNA damage-inducible transcript 3 protein (DDIT3; cat. no. 2895, 1:1,000 dilution), anti-eukaryotic translation initiation factor 2-α kinase 3 (EIF2AK3; cat. no. 3192, 1:1,000 dilution), anti-p-CDK substrate motif [(K/H)pSP] MultiMab™ (cat. no. 9477, 1:1,000 dilution), anti-CCNA2 (cat. no. 4656, 1:1,000 dilution), anti-CCNB1 (cat. no. 4138, 1:1,000 dilution), anti-autophagy protein 5 (ATG5; cat. no. 12994, 1:1,000 dilution), anti-RIPK1 (cat. no. 3493, 1:1,000 dilution), anti-ERBB2 (cat. no. 4290, 1:1,000 dilution), and anti-p-ERBB2 (Tyr1221/1222) (cat. no. 2243, 1:1,000 dilution) from Cell Signaling Technology (Danvers, MA, USA). Anti-CDK1 (A17) antibody was a kind gift from Dr J Gannon and Dr T Hunt (Francis Crick Institute, London, UK). The membranes were followed by incubation with horseradish peroxidase-conjugated secondary antibodies [anti-mouse immunoglobulin G (IgG); cat. no. 115-035-003; 1:5,000 dilution; or anti-rabbit IgG; cat. no. 711-035-152; 1:5,000 dilution; Jackson ImmunoResearch Laboratories, Inc., West Grove, PA, USA] for 1 h at room temperature. Immunoreactive proteins were detected with enhanced chemiluminescence reagent (Immobilon Western Chemiluminescent HRP Substrate; EMD Millipore). Densitometry analysis was performed using the WSE-6300 Luminograph III molecular imager (ATTO Corporation, Tokyo, Japan) and ATTO CS Analyzer 4 densitograph software (version 2.3.1, ATTO Corporation).

Gene expression analysis. Total RNA was extracted from A549 cells using a NucleoSpin RNA kit (Takara Bio, Inc., Otsu, Japan) and reverse transcribed to cDNA using PrimeScript RT Master mix (Takara Bio, Inc.) according to the manufacturer's instructions. The expression of ER stress-associated genes was determined by quantitative polymerase chain reaction (qPCR) using SYBR Premix Ex Taq II Tli RNase H Plus (Takara Bio, Inc.). The sequences of validated primers and reaction conditions were as follows (42,43): 5'-CCTAGCTGTGTCAGAATCTCCATC C-3' and 5'-GTTTCAATGTCACCATCCAAGATCC-3' for *HSPA5*; 5'-AAATCAGAGCTGGAACCTGAGGA-3' and 5'-CCATCTCTGCAGTTGGATCAGTC-3' for *DDIT3*; 5'-AACCAGCAGTTCCCTTCCTG-3' and 5'-TTGCCTCTC GCTCACCATAC-3' for protein phosphatase 1 regulatory subunit 15A (*PPP1R15A*); 5'-AAGTGCCGCACAGGG TGTCC-3' and 5'-GCTGGGACTTCCCCACTGTGC-3' for tumor necrosis factor receptor superfamily member 10B (*TNFRSF10B*); 5'-CCCGATCGTGAAGCAGTTAGA-3' and 5'-CAGAACCACCTTTATAGGTCCTGAA-3' for ER to nucleus signaling 1 *(ERN1)*; 5'-AAGCCCTGATGGTGC TAACTGAA-3' and 5'-CATGTCTATGAACCCATCCTC GAA-3' for activating transcription factor 6 (*ATF6*); and 5'-GCACCGTCAAGGCTGAGAAC-3' and 5'-TGGTGA AGACGCCAGTGGA-3' for *GAPDH*. qPCR was performed in a Thermal Cycler Dice Real-Time System TP800 (Takara Bio, Inc.) under the following conditions: Initial denaturation at 95˚C for 30 sec, followed by 45 cycles of the sequence of denaturation at 95˚C for 5 sec and simultaneous annealing and extension at 60˚C for 30 sec. Data were analyzed using Thermal Cycler Dice Real-Time System Software (Takara Bio, Inc.) and the comparative Cq method ($2^{-\Delta\Delta Cq}$) was used for relative quantification of gene expression (44). The data were standardized to *GAPDH* as an internal control.

Assessment of autophagy flux using the GFP-LC3-RFP-LC3ΔG system. A549/GFP-LC3-RFP-LC3ΔG cells ($8x10^3$ cells/well) were plated on a 96-well plate 24 h before treatment with FTY720. Fluorescence intensities derived from GFP-LC3B and RFP-LC3ΔG were monitored during the 24 h exposure to the drug, using an Incu-Cyte ZOOM cell imaging system (Essen BioScience, Ltd., Ann Arbor, MI, USA). Autophagy flux was measured as alterations in the relative intensities of GFP/RFP, using DMSO-treated groups as the control (45).

Lysotracker staining. A549 cells ($8x10^4$ cells/well) were seeded onto glass coverslips in a 24-well culture plate for 24 h. Next, A549 cells were treated with FTY720 or BafA1 for 4 h and then incubated for 30 min in 50 nM LysoTracker Red DND-99 (Molecular Probes; Thermo Fisher Scientific, Inc.). Coverslips were washed twice with PBS and cells were fixed in 2% paraformaldehyde for 10 min at room temperature. Following washing, the coverslips were mounted in ProLong Diamond Antifade Mountant (Thermo Fisher Scientific, Inc.). The cells were visualized using an LSM 700 confocal laser scanning fluorescence microscope (Zeiss GmbH, Jena, Germany) equipped with Plan-Apochromat 40x/1.4 oil DIC (Zeiss GmbH). All images were acquired and processed equally using ZEN 2012 software (version 8.1.0.484, Zeiss GmbH).

Cell cycle analysis. A549 cells ($1x10^6$ cells/100 mm dish) were plated on 100 mm dishes. After seeding for 24 h, A549 cells were treated with the indicated drugs for 24 h. The cells were harvested and fixed in 75% ethanol for 1 h at 4˚C. Next, the cells were treated with RNaseA (0.1 mg/ml) at 37˚C for 30 min and stained with propidium iodide (PI) (25 μg/ml) for 15 min at room temperature. DNA content was determined using Attune Acoustic Focusing Flow Cytometer (Applied Biosystems; Thermo Fisher Scientific, Inc.) and the cell cycle distribution was analyzed using ModFit LT version 5.0 (Verity Software House, Inc., Topsham, ME, USA).

Immunofluorescence analysis. A549 cells ($8x10^4$ cells/well) were seeded onto glass coverslips in a 24-well culture plate for 24 h. A549 cells were subsequently treated with FTY720 or FTY720-P for 1 or 4 h. Coverslips were washed twice with PBS and cells were fixed in 2% paraformaldehyde for 10 min at room temperature. Following washing, cells were permeabilized in 0.1% Triton X-100 for 5 min, followed by washing twice with PBS. The coverslips were blocked with 10% newborn calf serum (Gibco; Thermo Fisher Scientific, Inc., Waltham, MA, USA) for 1 h at room temperature, then incubated with a primary anti-sphingosine 1-phosphate receptor 1 (S1PR1) antibody (cat. no. ab11424; 1:200 dilution; Abcam, Cambridge, MA, USA) at 4˚C overnight. Following three washes, coverslips were incubated with Alexa Fluor 488-conjugated anti-Rabbit IgG (cat. no. A-11034; 1:1,000 dilution; Molecular Probes; Thermo Fisher Scientific, Inc.) and DAPI (1 μM; Sigma-Aldrich; Merck KGaA) at 37˚C for 1 h. Following washing, the coverslips were mounted in ProLong Diamond Antifade Mountant (Thermo Fisher Scientific, Inc.). Cells were visualized using an LSM 700 confocal laser scanning fluorescence microscope (Zeiss GmbH) equipped with Plan-Apochromat 40x/1.4 oil DIC (Zeiss GmbH) and

acquired images were analyzed using ZEN 2012 software (version 8.1.0.484; Zeiss GmbH).

May-Grünwald-Giemsa staining. A549 ($4x10^4$ cells/well) cells were seeded onto glass coverslips in a 24-well culture plate. After 24 h, the cells were treated with the indicated reagents for 24 or 48 h. Coverslips were washed twice with PBS and fixed in methanol for 10 min. These cells were stained with May-Grünwald's stain solution (Muto Pure Chemicals Co., Ltd., Tokyo Japan) for 3 min at room temperature. After adding equal volume of PBS, coverslips were left to stand for another 3 min. Once the May-Grünwald's stain solution was removed, the cells were stained with diluted (1:20 with water) Giemsa's stain solution (Muto Pure Chemicals Co., Ltd.) for 20 min at room temperature. After washing and drying, the cells were examined under a BZ-8100 digital microscope (Keyence Co., Osaka, Japan) equipped with PlanApo 20x NA0.75 (Nikon Corporation, Tokyo, Japan).

Knockout of ATG5 gene by CRISPR/Cas9-mediated genome editing. Target sequences for CRISPR interference for human *ATG5*, AACTTGTTTCACGCTATATC (exon 2) or AAGAGT AAGTTATTTGACGT (exon 3), were derived from a previous report (46). In total, two complementary oligonucleotides with *Bpi*I restriction sites for guide RNAs (gRNAs) were synthesized at FASMAC (Kanagawa, Japan), and cloned into the pX459 CRISPR/Cas9-Puro vector (Addgene, Inc., Cambridge, MA, USA) deposited by the Feng Zhang Laboratory. A549 cells ($2x10^6$ cells/100 mm dish) were transfected with pX459-gRNA using Lipofectamine® 3000 according to the manufacturer's instructions. The day after transfection, cells were treated with 2 μg/ml puromycin for 2 days. Surviving cells were diluted in growth medium (RPMI-1640 medium supplemented with 10% heat inactivated fetal bovine serum) to prepare cell suspension (5 cells/ml) and distributed in 100 μl of the cell suspension per well in a 96-well plate. The expression of ATG5 in the expanded colonies was detected by immunoblotting using anti-ATG5 antibody (cat. no. 12994; 1:1,000 dilution) at 4˚C overnight to select the ATG5-depleted colonies. The genome sequences of the edited locus in selected colonies were also confirmed by Sanger DNA sequencing performed at FASMAC, which demonstrated that the expected deletion and frameshifting were present in each exon of *ATG5*.

Gene silencing of RIPK1. A549 cells ($2x10^6$ cells/100 mm dish) were transfected with either a control small interfering RNA (siRNA; 15 nM; cat. no. 46-2001; Thermo Fisher Scientific, Inc.) or Stealth siRNA (15 nM) targeting human *RIPK1* (HSS112847; cat. no. 10620318; Thermo Fisher Scientific, Inc.) using Lipofectamine RNAiMAX (Thermo Fisher Scientific, Inc.) according to the manufacturer's instructions. A total of 24 h post-transfection, these cells were re-plated on a 96-well plate for cell viability assays.

Statistical analysis. All data are shown as the mean ± standard deviation. Statistical analysis was performed using a one-way analysis of variance (ANOVA), followed by Dunnett's post hoc test for comparisons with a control group, or with the Student-Newman-Keuls post hoc test for multiple comparisons between all pairs of groups. These statistical analyses were performed using Excel Statistical Program File ystat2008 (Igakutosho-shuppan, Ltd., Tokyo, Japan). $P<0.01$ was considered to indicate a statistically significant difference.

Table I. IC_{50} values of the drugs used in this study in A549 cells.

Drugs	IC_{50} (μM)
Sorafenib	11.1
Gefitinib	25.6
Erlotinib	>40
Lapatinib	21.7
Imatinib	>40
FTY720	10.5
FTY720-P	ND

ND, not determined.

Results and discussion

Cell growth inhibition in NSCLC cells after single or combined treatment with TKIs and FTY720. A549 cells, expressing wild-type EGFR, were treated with different concentrations (0-40 μM) of the TKIs Sor, Gef, Erl, Lap, and Ima (Fig. 1A). The half-maximal inhibition concentration (IC_{50}) values of each tested compound were shown in Table I. Sor markedly decreased A549 cell viability in a dose- and time-dependent manner. The effectiveness of Sor may be attributable to the activating KRAS proto-oncogene, GTPase (*KRAS*) mutations in A549 cells (47). A target molecule of Sor is Raf kinase, a downstream effector molecule of KRAS (48). In contrast, Gef, Erl, and Lap only slightly decreased A549 cell viability, while Ima showed nearly no effects on A549 cell viability.

Treatment with 15 μM FTY720 resulted in apparent cytotoxicity, although FTY720 at a concentration of ≤5 μM showed no cytotoxicity (Fig. 1B). It is well known that one of the biological effects of FTY720 is attributed to its phosphorylated form, FTY720-P: It strongly binds to S1PR1, inducing the internalization and degradation of S1PR1 at submicromolar concentrations (19,25). However, in the current study, the cytocidal activity of FTY720 in A549 cells was observed only at micromolar concentrations, and FTY720-P was not found to be cytocidal (Fig. 1B). In addition, most S1PR1 molecules were localized in the nucleus in A549 cells and the localization of S1PR1 did not change following treatment with FTY720 or FTY720-P (Fig. S1). Therefore, FTY720-mediated cytotoxicity in A549 cells was not attributed to its phosphorylated form, FTY720-P.

Next, the effects of combined treatment with TKIs and FTY720 was evaluated. It was found that the combined treatment with Lap or Sor and FTY720 effectively enhanced A549 cell cytotoxicity (Fig. 1C). To determine what type of combinatory effect was exerted, the combination index (CI) values were calculated. Specifically, CI <1, CI=1, and CI >1 indicate synergistic, additive and antagonistic effects, respectively (49). The CI value of combined treatment with Sor (10 μM) and FTY720 (10 μM) was 0.74, and that

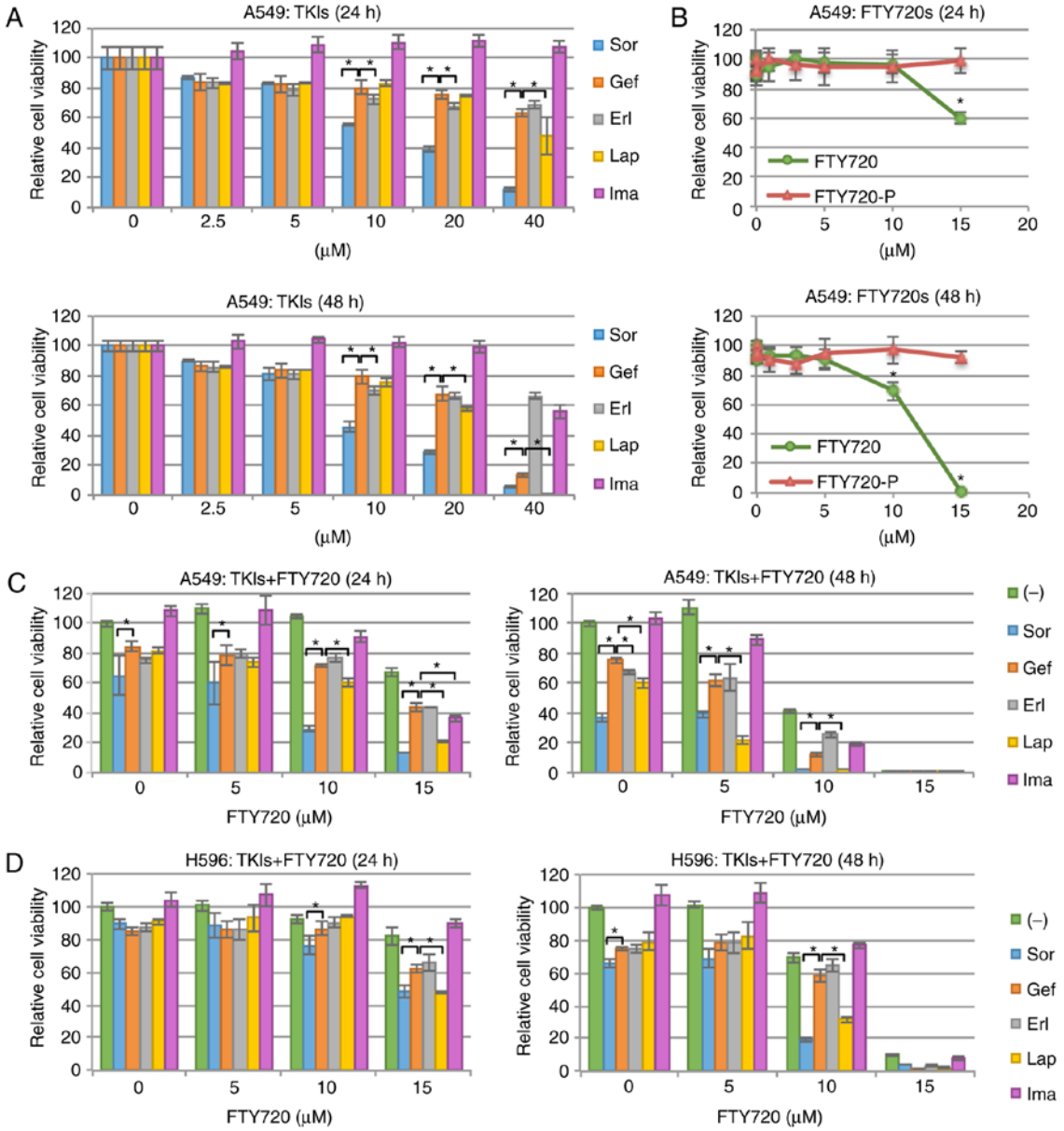

Figure 1. Cell growth inhibition in NSCLC cells. Cell viability was assessed at 24 and 48 h following treatment with the indicated drug. (A) A549 cells were treated with one of the following tyrosine kinase inhibitors: Sor, Gef, Erl, Lap or Ima, at the indicated concentrations. *P<0.01 vs. treatment with Gef. Gef-treated group were used for comparisons because Gef is a well-known tyrosine kinase inhibitors for the treatment of non-small cell lung cancer. (B) A549 cells were treated with FTY720 or FTY720-P at the indicated concentrations. *P<0.01 vs. 0 μM. (C) A549 cells were treated with FTY720 at the indicated concentrations, combined with Sor, Gef, Erl, Lap or Ima (at 10 μM). *P<0.01 vs. combined treatment with Gef and FTY720. (D) H596 cells were also treated with reagents and cell viability was assessed. *P<0.01 vs. combined treatment with Gef and FTY720. Sor, sorafenib; Gef, gefitinib; Erl, erlotinib; Lap, lapatinib; Ima, imatinib; FTY720-P, FTY720 (S)-phosphate.

of Lap (10 μM) and FTY720 (10 μM) was 0.77 (data not shown); therefore, both combinations showed synergistic effects on A549 cells. In contrast, FTY720 only marginally enhanced Gef- or Erl-induced cytotoxicity (Fig. 1C). This synergistic effect of Lap and FTY720 or Sor and FTY720 was also observed in another NSCLC cell line H596, which also expresses wild-type EGFR (Fig 1D). These data demonstrated that the cytotoxicity of NSCLC cells with wild-type *EGFR* was increased following combined treatment with Lap or Sor and FTY720.

Changes of autophagy flux in NSCLC cells following treatment with FTY720. As described above, it has been previously reported that macrolide antibiotics suppress autophagy flux and promote the cytotoxic effects of TKIs in various cancer cell lines, including A549 (38,50). Therefore, whether the modulation of autophagy flux was involved in the enhanced cytotoxicity exerted by FTY720 was examined. Treating A549 cells with each TKI resulted in an increased expression of MAP1LC3B-II, a lipidated form of MAP1LC3B, which is a hallmark of autophagosome formation (51) (Fig. 2A). Additionally, SQSTM1, a substrate of autophagy (51), decreased in response to Sor treatment and accumulated in response to Gef, Lap, or Ima treatment (Fig. 2A). These results suggested that Sor induced autophagy flux and Gef, Lap or Ima suppressed autophagy flux in A549 cells. Treating A549

cells with FTY720 resulted in an increased expression of MAP1LC3B-II and an accumulation of SQSTM1 (Fig. 2B). In addition, treatment with BafA1, a well-known lysosomal inhibitor (52), also increased the expression of MAP1LC3B-II, by blocking the catabolic flux of autophagy. However, combined treatment with FTY720 and BafA1 failed to further increase MAP1LC3B-II expression, compared with the treatment with either FTY720 or BafA1 alone (Fig. 2B). This result indicated that FTY720 suppressed autophagy flux, but does not induce autophagy.

To analyze the autophagy flux, a GFP-LC3-RFP-LC3ΔG-based system was used (45). GFP-LC3-RFP-LC3ΔG is cleaved into equimolar amounts of GFP-LC3 and RFP-LC3ΔG. GFP-LC3 is degraded by autophagy, while RFP-LC3ΔG remains in the cytosol, functioning as an internal control. Thus, autophagy flux can be estimated by calculating the GFP/RFP signal ratio. In the present study, FTY720 or Lap evidently suppressed autophagy flux in a dose-dependent manner, as indicated by an increased GFP/RFP ratio, whereas Sor induced autophagy flux in a dose-dependent manner, as shown by a reduced GFP/RFP ratio (Fig. 2C). These results, namely that Lap-mediated autophagy suppression and Sor-mediated autophagy induction, obtained in A549 cells were consistent with a previous study in HeLa cells (45). Alterations in autophagy flux after treatment with Gef, Erl, or Ima were small and were not dose-dependent (data not shown).

Furthermore, the effects of FTY720 on lysosomes using LysoTracker dye were investigated, which stains lysosomes and other acidic organelles. After treatment with FTY720 or BafA1 for 4 h, the intensity of LysoTracker dye was clearly decreased (Fig. 2D). This suggested that FTY720 inhibited the acidification of lysosomes and autolysosomes, limiting protein degradation in these organelles and subsequently inhibiting autophagy flux.

ER stress loading in NSCLC cells after combined treatment with TKIs and FTY720. During the inhibition of intracellular proteolytic processes, ER stress loading is pronounced, which reduces cell proliferation and viability (43,53,54). Because FTY720 suppressed autophagy flux (Fig. 2), whether ER stress loading was involved in the enhanced cytotoxicity resulting from combination treatment with FTY720 was investigated (Fig. 3A). Expression of ER stress-associated proteins such as HSPA5 and DDIT3 was upregulated in response to single treatment with Sor, but not with Gef or Lap. However, combined treatment with Lap and 10 μM FTY720 markedly upregulated the expression of these proteins, although single treatment of FTY720 had no effects on protein expression. Additionally, combined treatment of Lap with 5 μM FTY720 minimally upregulated the expression of these proteins, indicating that the expression of ER stress-associated proteins was dependent on the concentration of FTY720, similar to cell viability. Furthermore, following combined treatment with Lap and FTY720, a mobility shift of EIF2AK3, an ER stress sensor protein, was detected (Fig. 3A), likely as a result of its phosphorylation and activation (55).

qPCR data for *HSPA5* and *DDIT3* expression supported the immunoblotting data (Fig. 3B). Additionally, DDIT3-regulated genes such as *PPP1R15A* and *TNFRSF10B* showed similar regulation in response to Sor, Lap and FTY720 treatment. Furthermore, the expression of the ER stress sensor genes, *ERN1* and *ATF6* was upregulated after treatment with Sor alone and after the combined treatment with Lap or Sor and FTY720. Taken together, these data demonstrated that ER stress loading was enhanced following treatment with Sor alone or in combination with FTY720, as well as in response to Lap and FTY720 combined treatment, suggesting that ER stress loading was involved in enhancing the cytotoxicity exerted by the combination treatment with FTY720.

Cytostatic effects on NSCLC cells after combined treatment with TKIs and FTY720. It has been reported that the exposure of cells to ER stress loading leads to the activation of EIF2AK3, phosphorylation of eIF2α, and subsequent repression of cyclin D translation, resulting in cell cycle arrest (40,56-59). Therefore, whether combination treatment with FTY720 induced cytostatic effects in NSCLC cells was examined. The protein expression of CCND1/D3 and CDK4/6 was suppressed after the treatment with Sor alone and following combined treatment with Lap and FTY720 (Fig. 4A). Additionally, the protein expression of CCNA2, CCNB1, and CDK1, which are regulators for G_2/M phase of the cell cycle, was also suppressed, particularly following combined treatment with Sor and FTY720, or Lap and FTY720 (Fig. 4B). Furthermore, the expression of phosphorylated CDK substrate motif was also reduced in response to these drugs (Fig. 4C). Whether cell cycle progression was affected by the combined treatments was further investigated. Fig. 4D showed that combined treatment with Lap and FTY720 or Sor and FTY720 caused significant accumulation of A549 cells in G_0/G_1 and G_2/M phases, with a concomitant decrease in the number of cells in S phase (non-treated, 34.8%; Sor and FTY720, 14.7%; Lap and FTY720, 5.7%). These data indicated that combined treatment with Lap and FTY720 or Sor and FTY720 exerted cytostatic effects on NSCLC cells; these effects were associated with the expression of ER stress-associated proteins and A549 cell viability.

EGFR TKIs are standard first-line therapies for patients with advanced NSCLC with activating *EGFR* mutations. However, it is essential to identify additional therapeutic strategies to block the growth of NSCLC in patients with wild-type *EGFR*. In our previous study, it was demonstrated that macrolide antibiotics enhance the cytotoxic effect of Gef in NSCLC cells; however, a relatively high dose of Gef (25 μM) was required to achieve these synergistic effects (38). In order to discover novel effective combination treatments, the effects of various TKIs combined with FTY720 were investigated in *EGFR* wild-type NSCLC cells. The current study showed that FTY720 enhanced the cytotoxicity of TKIs (10 μM), particularly Lap and Sor, whereas the macrolide antibiotic azithromycin only minimally enhanced the TKI-mediated cytotoxicity (Fig. S2).

It was shown that FTY720 or Lap alone suppressed autophagy flux, whereas Sor induced autophagy flux. To investigate whether the suppression of autophagy flux by FTY720 was required to exert the synergistic cytotoxicity of FTY720 and TKIs, *ATG5*-knockout A549 cells were generated. It was confirmed that conversion of MAP1LC3B-I to MAP1LC3B-II-a critical step in the formation of autophagosomes-was completely abolished in

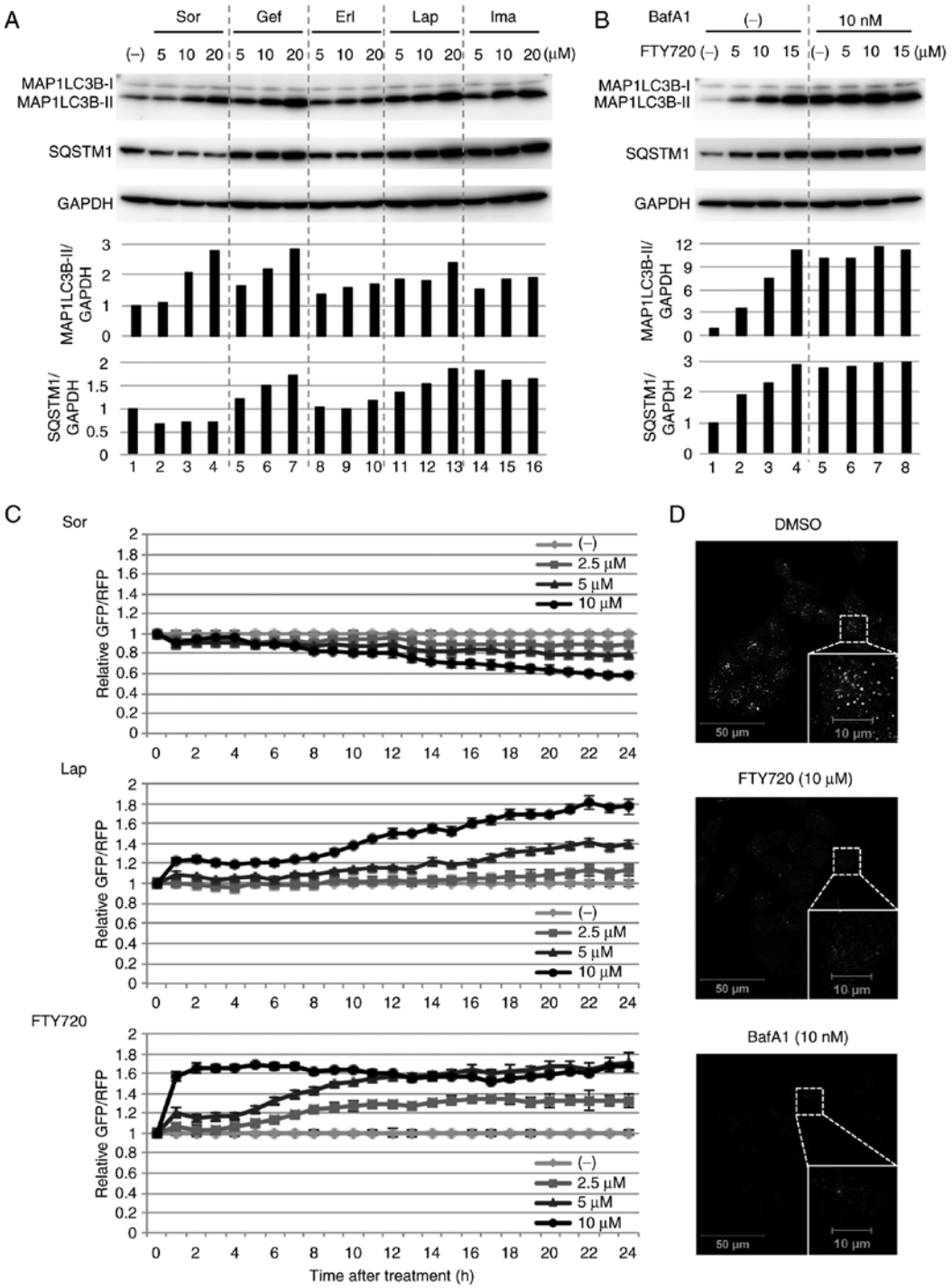

Figure 2. Alterations in autophagy flux. (A) A549 cells were treated with Sor, Gef, Erl, Lap or Ima at the indicated concentrations for 24 h, and with (B) FTY720 and BafA1 for 24 h at the indicated concentrations. The immunoblots show MAP1LC3B and SQSTM1 expression. GAPDH was used as an internal control. Band intensities were determined by densitometry and the ratios of MAP1LC3B-II/GAPDH and SQSTM1/GAPDH are presented. Representative data from multiple experiments are shown. (C) A549/GFP-LC3-RFP-LC3ΔG cells were treated with Sor, Lap or FTY720 at the indicated concentrations. Fluorescence intensities derived from GFP-LC3B and RFP-LC3ΔG were monitored over 24 h. Autophagy flux was assessed as alterations in the relative intensities of GFP/RFP, using DMSO-treated groups as a control. (D) A549 cells were treated with FTY720 (10 μM) or BafA1 (10 nM) for 4 h and stained with 50 nM LysoTracker Red DND-99. All images were acquired and processed equally. Sor, sorafenib; Gef, gefitinib; Erl, erlotinib; Lap, lapatinib; Ima, imatinib; DMSO, dimethyl sulfoxide; GFP, green fluorescent protein; RFP, red fluorescent protein; MAP1LC3B, microtubule-associated proteins 1A/1B light chain 3B; SQSTM1, sequestosome; BafA1, bafilomycin A1.

ATG5-depleted colonies, even in the presence of BafA1, by immunoblotting using anti-MAP1LC3B antibody (Fig. S3). The results showed that FTY720 and/or TKIs exert a similar effect in *ATG5*-knockout and parental A549 cells (Fig. S3), suggesting that the suppression of autophagy flux by FTY720 was dispensable for synergistic cytotoxicity of FTY720 and TKIs. However, since an ATG5-independent autophagy pathway has also been reported (60,61), further experiments are needed to clarify the necessity of the autophagy flux modulation.

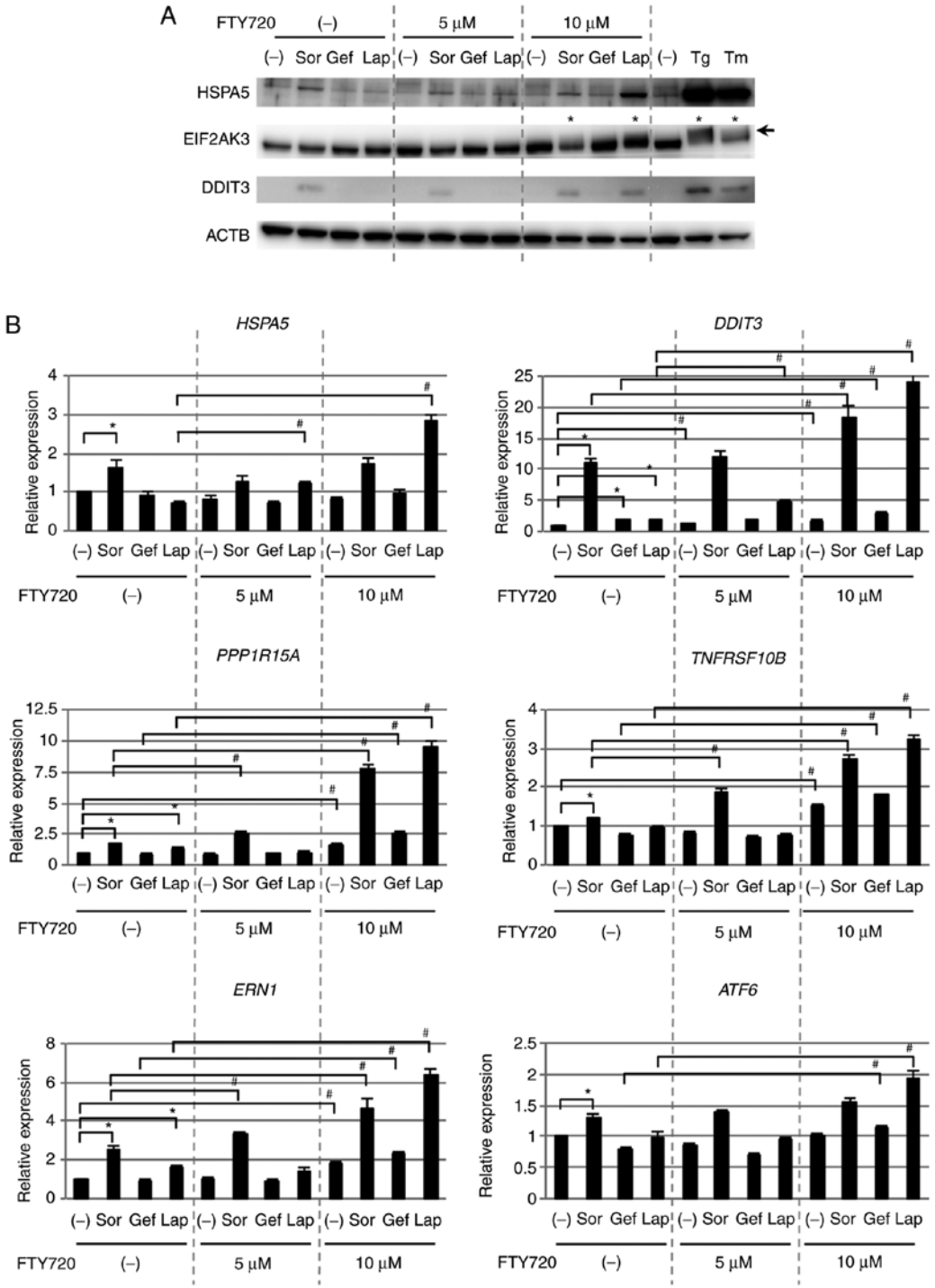

Figure 3. ER stress loading in NSCLC cells. (A) A549 cells were treated with one of the following tyrosine kinase inhibitors (10 μM): Sor, Gef, or Lap in the absence or presence of FTY720 (5 or 10 μM) for 24 h. Immunoblots showing expression of HSPA5, EIF2AK3, and DDIT3. ACTB was used as an internal control. Tg and Tm were used to induce ER stress as positive control reagents. The arrow indicates the position of shifted EIF2AK3 bands. Asterisks show lanes in which shifted EIF2AK3 bands were detected. (B) A549 cells were treated as in Fig. 3A, and ER stress-associated gene expression was determined by quantitative polymerase chain reaction analysis and normalized to *GAPDH*. The expression level of each gene in dimethyl sulfoxide-treated cells was designated as 1.0. *P<0.01 vs. non-treated only in the absence of FTY720; $^{\#}$P<0.01 vs. each TKI-treated in the absence of FTY720. Sor, sorafenib; Gef, gefitinib; Erl, erlotinib; Lap, lapatinib; Ima, imatinib; Tg, thapsigargin; Tm, tunicamycin; ER, endoplasmic reticulum; HSPA5, heat shock protein family A member 5; EIF2AK3, eukaryotic translation initiation factor 2-α kinase 3; DDIT3, DNA damage-inducible transcript 3 protein; ACTB, β-actin.

Notably, although FTY720 enhanced the cytotoxicity of Lap or Sor, no evident morphological apoptotic features, such as nuclear fragmentation and apoptotic body formation, were detected (Fig. S4). Additionally, the decreased cell viability observed following combined treatment with TKIs and FTY720 was not suppressed by co-treatment with the apoptosis inhibitor Z-VAD-FMK or necroptosis inhibitor necrostatin-1 (Fig. S5). Furthermore, the transient siRNA-mediated knockdown of *RIPK1*, an indispensable regulator for necroptosis, did not affect cell sensitivity to

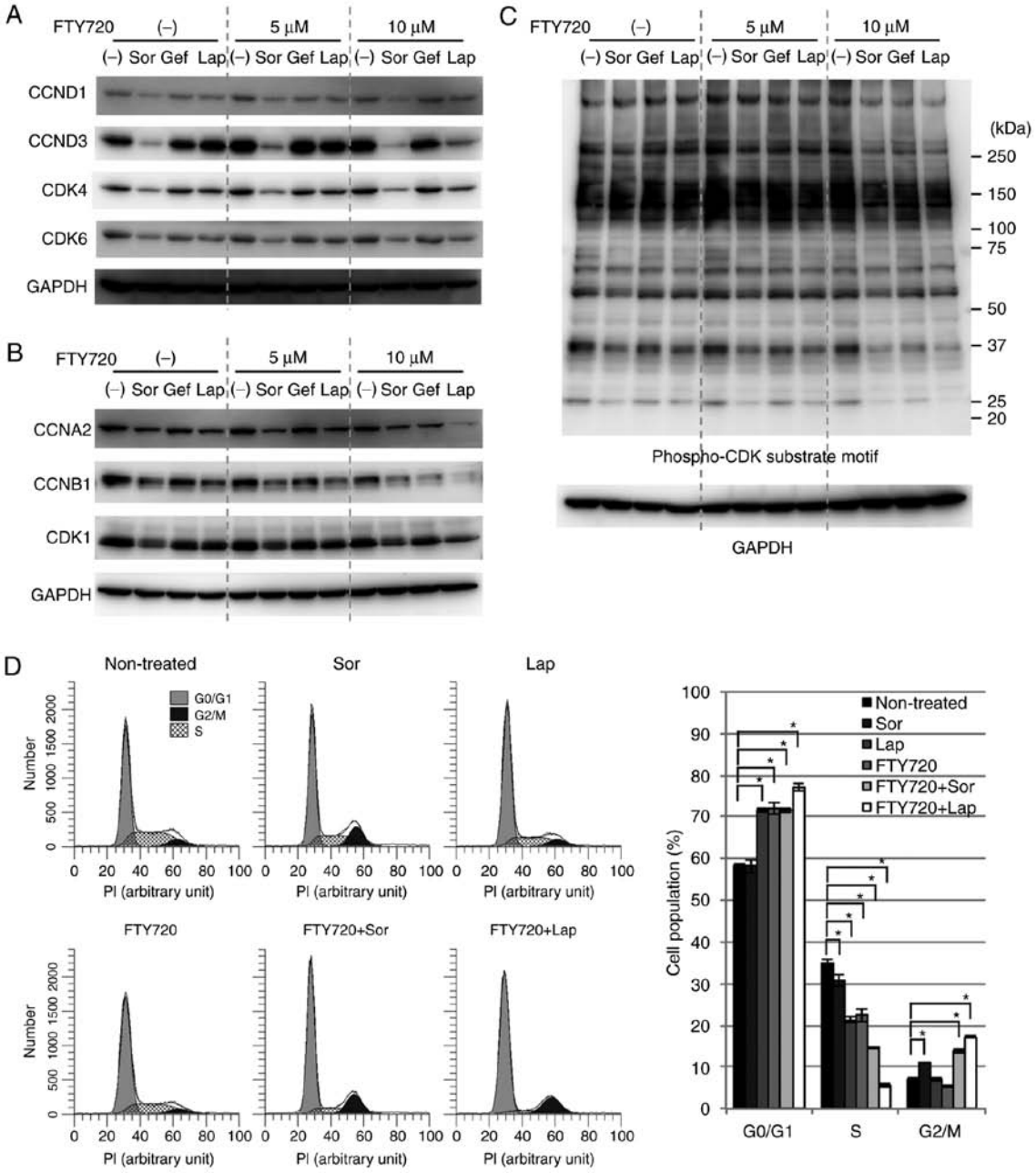

Figure 4. Cytostatic effects on NSCLC cells. A549 cells were treated with one of the following tyrosine kinase inhibitors (10 μM): Sor, Gef, or Lap in the absence or presence of FTY720 (5 or 10 μM) for 24 h. Immunoblots showing the expression of (A) CCND1, CCND3, CDK4, CDK6, (B) CCNA2, CCNB1 and CDK1, as well as (C) proteins containing the phosphorylated CDK substrate motif. GAPDH was used as an internal control. (D) A549 cells were treated with Sor (10 μM) or Lap (10 μM) in the presence or absence of FTY720 (10 μM) for 24 h. Cells were stained with PI prior to analysis using a flow cytometer. Cell cycle distribution was analyzed using ModFit LT version 5.0. *P<0.01 vs. non-treated cells in each phase. PI, propidium iodide; CCN, cyclin; CDK, cyclin-dependent kinase; Sor, sorafenib; Gef, gefitinib; Lap, lapatinib; NSCLC, non-small cell lung cancer.

TKIs combined with FTY720 in A549 cells (Fig. S6). Several lines of research using A549 cells have reported Sor-induced apoptosis, Lap-induced apoptosis or FTY-induced necroptosis (62-64); however, in the present study, typical features of apoptosis or necroptosis were not found in A549 cells treated with a combination of TKIs and FTY720. All these data suggest that further experiments are required in order to clarify the mechanisms of cell death induced by combined treatment with TKIs and FTY720.

It is also necessary to consider that, although FTY720 markedly enhanced Lap-mediated cytotoxicity (Fig. 1C and D, and Fig. S7), the enhanced effects of FTY720 on Gef or Erl were less pronounced (Fig. 1C and D). Gef and Erl inhibit the phosphorylation of EGFR. In contrast, Lap inhibits the phosphorylation of ERBB2 and EGFR (65). Therefore, the differences in the enhanced effects of FTY720 may be due to its effects on ERBB2. However, the expression of ERBB2 and phosphorylated ERBB2 were not detected in A549, H596 and H226 cells (Fig. S8). Additionally, it has been previously reported that FTY720 decreases the sensitivity to Lap in SKBR3 cells, an ERBB2-overexpressing breast cancer cell line (66). Therefore, further studies are needed to determine the underlying molecular mechanism of the combined effects of Lap and FTY720.

In conclusion, it was shown that the cytotoxic effects of Lap and Sor against *EGFR* wild-type NSCLC cells were markedly enhanced by the combined treatment with FTY720, making FTY720 a strong candidate for improving the efficacy of Lap treatment in NSCLC patients with wild-type *EGFR*. Sor is another good candidate for improving the therapeutic options, either as a single drug or in combination with FTY720. There are many existing drugs with new therapeutic indications (e.g. the anti-osteoporotic drug raloxifene for breast cancer and the anti-inflammatory/analgesic drug aspirin for colorectal cancer), which have been already evaluated in terms of safety and toxicity (37); therefore, the present study has the possibility to rapidly improve the treatment of NSCLC patients with wild-type *EGFR*. Additionally, the benefits in NSCLC patients with activating *EGFR* mutations resulting from treatment with EGFR TKIs are often limited by the eventual development of resistance to these agents (67,68). The present study could be useful to increase the treatment benefits in such patients.

Acknowledgements

The authors would like to thank Dr Noboru Mizushima (The University of Tokyo, Graduate School and Faculty of Medicine, Tokyo, Japan) for gifting the GFP-LC3-RFP-LC3ΔG plasmid, and Dr J Gannon and Dr T Hunt (The Francis Crick Institute, London, UK) for gifting of the anti-CDK1 (A17) antibody. The authors would also like to thank Dr Akihisa Abe, Ms. Ayako Hirota, Ms. Yumiko Yamada, and Ms. Mayumi Tokuhisa for their technical assistance and Editage (www.editage.jp) for English language editing.

Funding

This study was supported by funds provided through the MEXT-Supported program of the Strategic Research Foundation at Private Universities (grant no. S1411011; 2014-2018) from the Ministry of Education, Culture, Sports, Science and Technology of Japan to KM, and Research Funding granted by the Tokyo Medical University President to MH.

Availability of data and materials

All data generated or analyzed during this study are available from the corresponding author on reasonable request.

Authors' contributions

MH and KM designed the present study. KO, TO, ADL, AY, HH, HK, SM, NT, and MH performed the experiments and analyzed the data. MH, KO, NT, and KM were major contributors in writing the manuscript. All authors read and approved the final manuscript.

Ethics approval and consent to participate

Not applicable.

Patent consent for publication

Not applicable.

Competing interests

The authors declare that they have no competing interests.

References

1. Torre LA, Siegel RL and Jemal A: Lung cancer statistics. Adv Exp Med Biol 893: 1-19, 2016.
2. Siegel RL, Miller KD and Jemal A: Cancer statistics, 2018. CA Cancer J Clin 68: 7-30, 2018.
3. Pao W and Girard N: New driver mutations in non-small-cell lung cancer. Lancet Oncol 12: 175-180, 2011.
4. Govindan R, Ding L, Griffith M, Subramanian J, Dees ND, Kanchi KL, Maher CA, Fulton R, Fulton L, Wallis J, *et al*: Genomic landscape of non-small cell lung cancer in smokers and never-smokers. Cell 150: 1121-1134, 2012.
5. Imielinski M, Berger AH, Hammerman PS, Hernandez B, Pugh TJ, Hodis E, Cho J, Suh J, Capelletti M, Sivachenko A, *et al*: Mapping the hallmarks of lung adenocarcinoma with massively parallel sequencing. Cell 150: 1107-1120, 2012.
6. Devarakonda S, Morgensztern D and Govindan R: Genomic alterations in lung adenocarcinoma. Lancet Oncol 16: e342-e351, 2015.
7. Chapman AM, Sun KY, Ruestow P, Cowan DM and Madl AK: Lung cancer mutation profile of EGFR, ALK, and KRAS: Meta-analysis and comparison of never and ever smokers. Lung Cancer 102: 122-134, 2016.
8. Gibelin C and Couraud S: Somatic alterations in lung cancer: Do environmental factors matter? Lung Cancer 100: 45-52, 2016.
9. Hirsch FR, Scagliotti GV, Mulshine JL, Kwon R, Curran WJ Jr, Wu YL and Paz-Ares L: Lung cancer: Current therapies and new targeted treatments. Lancet 389: 299-311, 2017.
10. Okabe T, Okamoto I, Tamura K, Terashima M, Yoshida T, Satoh T, Takada M, Fukuoka M and Nakagawa K: Differential constitutive activation of the epidermal growth factor receptor in non-small cell lung cancer cells bearing *EGFR* gene mutation and amplification. Cancer Res 67: 2046-2053, 2007.
11. Ono M and Kuwano M: Molecular mechanisms of epidermal growth factor receptor (EGFR) activation and response to gefitinib and other EGFR-targeting drugs. Clin Cancer Res 12: 7242-7251, 2006.
12. Lynch TJ, Bell DW, Sordella R, Gurubhagavatula S, Okimoto RA, Brannigan BW, Harris PL, Haserlat SM, Supko JG, Haluska FG, *et al*: Activating mutations in the epidermal growth factor receptor underlying responsiveness of non-small-cell lung cancer to gefitinib. N Engl J Med 350: 2129-2139, 2004.
13. Taron M, Ichinose Y, Rosell R, Mok T, Massuti B, Zamora L, Mate JL, Manegold C, Ono M, Queralt C, *et al*: Activating mutations in the tyrosine kinase domain of the epidermal growth factor receptor are associated with improved survival in gefitinib-treated chemorefractory lung adenocarcinomas. Clin Cancer Res 11: 5878-5885, 2005.
14. Lee JK, Hahn S, Kim DW, Suh KJ, Keam B, Kim TM, Lee SH and Heo DS: Epidermal growth factor receptor tyrosine kinase inhibitors vs conventional chemotherapy in non-small cell lung cancer harboring wild-type epidermal growth factor receptor: A meta-analysis. JAMA 311: 1430-1437, 2014.
15. Nan X, Xie C, Yu X and Liu J: EGFR TKI as first-line treatment for patients with advanced EGFR mutation-positive non-small-cell lung cancer. Oncotarget 8: 75712-75726, 2017.
16. Fogli S, Polini B, Del Re M, Petrini I, Passaro A, Crucitta S, Rofi E and Danesi R: EGFR-TKIs in non-small-cell lung cancer: Focus on clinical pharmacology and mechanisms of resistance. Pharmacogenomics 19: 727-740, 2018.
17. Zhou Y, Li S, Hu YP, Wang J, Hauser J, Conway AN, Vinci MA, Humphrey L, Zborowska E, Willson JK, *et al*: Blockade of EGFR and ErbB2 by the novel dual EGFR and ErbB2 tyrosine kinase inhibitor GW572016 sensitizes human colon carcinoma GEO cells to apoptosis. Cancer Res 66: 404-411, 2006.
18. Liu L, Cao Y, Chen C, Zhang X, McNabola A, Wilkie D, Wilhelm S, Lynch M and Carter C: Sorafenib blocks the RAF/MEK/ERK pathway, inhibits tumor angiogenesis, and induces tumor cell apoptosis in hepatocellular carcinoma model PLC/PRF/5. Cancer Res 66: 11851-11858, 2006.
19. Chiba K, Kataoka H, Seki N, Shimano K, Koyama M, Fukunari A, Sugahara K and Sugita T: Fingolimod (FTY720), sphingosine 1-phosphate receptor modulator, shows superior efficacy as compared with interferon-beta in mouse experimental autoimmune encephalomyelitis. Int Immunopharmacol 11: 366-372, 2011.

20. Sonoda Y, Yamamoto D, Sakurai S, Hasegawa M, Aizu-Yokota E, Momoi T and Kasahara T: FTY720, a novel immunosuppressive agent, induces apoptosis in human glioma cells. Biochem Biophys Res Commun 281: 282-288, 2001.
21. Azuma H, Takahara S, Ichimaru N, Wang JD, Itoh Y, Otsuki Y, Morimoto J, Fukui R, Hoshiga M and Ishihara T: Marked prevention of tumor growth and metastasis by a novel immunosuppressive agent, FTY720, in mouse breast cancer models. Cancer Res 62: 1410-1419, 2002.
22. Lee TK, Man K, Ho JW, Sun CK, Ng KT, Wang XH, Wong YC, Ng IO, Xu R and Fan ST: FTY720 induces apoptosis of human hepatoma cell lines through PI3-K-mediated Akt dephosphorylation. Carcinogenesis 25: 2397-2405, 2004.
23. Schmid G, Guba M, Papyan A, Ischenko I, Brückel M, Bruns CJ, Jauch KW and Graeb C: FTY720 inhibits tumor growth and angiogenesis. Transplant Proc 37: 110-111, 2005.
24. Zhang L, Wang HD, Ji XJ, Cong ZX, Zhu JH and Zhou Y: FTY720 for cancer therapy (Review). Oncol Rep 30: 2571-2578, 2013.
25. White C, Alshaker H, Cooper C, Winkler M and Pchejetski D: The emerging role of FTY720 (Fingolimod) in cancer treatment. Oncotarget 7: 23106-23127, 2016.
26. Zhang N, Qi Y, Wadham C, Wang L, Warren A, Di W and Xia P: FTY720 induces necrotic cell death and autophagy in ovarian cancer cells: A protective role of autophagy. Autophagy 6: 1157-1167, 2010.
27. Liao A, Hu R, Zhao Q, Li J, Li Y, Yao K, Zhang R, Wang H, Yang W and Liu Z: Autophagy induced by FTY720 promotes apoptosis in U266 cells. Eur J Pharm Sci 45: 600-605, 2012.
28. Zhang L, Wang H, Ding K and Xu J: FTY720 induces autophagy-related apoptosis and necroptosis in human glioblastoma cells. Toxicol Lett 236: 43-59, 2015.
29. Li J, Wang SW, Zhang DS, Sun Y, Zhu CY, Fei Q, Hu J, Zhang C and Sun YM: FTY720-induced enhancement of autophagy protects cells from FTY720 cytotoxicity in colorectal cancer. Oncol Rep 35: 2833-2842, 2016.
30. Alinari L, Mahoney E, Patton J, Zhang X, Huynh L, Earl CT, Mani R, Mao Y, Yu B, Quinion C, *et al*: FTY720 increases CD74 expression and sensitizes mantle cell lymphoma cells to milatuzumab-mediated cell death. Blood 118: 6893-6903, 2011.
31. Ahmed D, de Verdier PJ, Ryk C, Lunqe O, Stal P and Flygare J: FTY720 (Fingolimod) sensitizes hepatocellular carcinoma cells to sorafenib-mediated cytotoxicity. Pharmacol Res Perspect 3: e00171, 2015.
32. Tay KH, Liu X, Chi M, Jin L, Jiang CC, Guo ST, Verrills NM, Tseng HY and Zhang XD: Involvement of vacuolar H(+)-ATPase in killing of human melanoma cells by the sphingosine kinase analogue FTY720. Pigment Cell Melanoma Res 28: 171-183, 2015.
33. Li X, Wang MH, Qin C, Fan WH, Tian DS and Liu JL: Fingolimod suppresses neuronal autophagy through the mTOR/p70S6K pathway and alleviates ischemic brain damage in mice. PLoS One 12: e0188748, 2017.
34. Levy JMM, Towers CG and Thorburn A: Targeting autophagy in cancer. Nat Rev Cancer 17: 528-542, 2017.
35. Ashburn TT and Thor KB: Drug repositioning: Identifying and developing new uses for existing drugs. Nat Rev Drug Discov 3: 673-683, 2004.
36. Jahchan NS, Dudley JT, Mazur PK, Flores N, Yang D, Palmerton A, Zmoos AF, Vaka D, Tran KQ, Zhou M, *et al*: A drug repositioning approach identifies tricyclic antidepressants as inhibitors of small cell lung cancer and other neuroendocrine tumors. Cancer Discov 3: 1364-1377, 2013.
37. Pushpakom S, Iorio F, Eyers PA, Escott KJ, Hopper S, Wells A, Doig A, Guilliams T, Latimer J, McNamee C, *et al*: Drug repurposing: Progress, challenges and recommendations. Nat Rev Drug Discov, 2018.
38. Sugita S, Ito K, Yamashiro Y, Moriya S, Che XF, Yokoyama T, Hiramoto M and Miyazawa K: EGFR-independent autophagy induction with gefitinib and enhancement of its cytotoxic effect by targeting autophagy with clarithromycin in non-small cell lung cancer cells. Biochem Biophys Res Commun 461: 28-34, 2015.
39. Wang M and Kaufman RJ: The impact of the endoplasmic reticulum protein-folding environment on cancer development. Nat Rev Cancer 14: 581-597, 2014.
40. McConkey DJ: The integrated stress response and proteotoxicity in cancer therapy. Biochem Biophys Res Commun 482: 450-453, 2017.
41. Wang M, Law ME, Castellano RK and Law BK: The unfolded protein response as a target for anticancer therapeutics. Crit Rev Oncol Hematol 127: 66-79, 2018.
42. Kawaguchi T, Miyazawa K, Moriya S, Ohtomo T, Che XF, Naito M, Itoh M and Tomoda A: Combined treatment with bortezomib plus bafilomycin A1 enhances the cytocidal effect and induces endoplasmic reticulum stress in U266 myeloma cells: Crosstalk among proteasome, autophagy-lysosome and ER stress. Int J Oncol 38: 643-654, 2011.
43. Moriya S, Che XF, Komatsu S, Abe A, Kawaguchi T, Gotoh A, Inazu M, Tomoda A and Miyazawa K: Macrolide antibiotics block autophagy flux and sensitize to bortezomib via endoplasmic reticulum stress-mediated CHOP induction in myeloma cells. Int J Oncol 42: 1541-1550, 2013.
44. Livak KJ and Schmittgen TD: Analysis of relative gene expression data using real-time quantitative PCR and the $2^{-\Delta\Delta C_T}$ method. Methods 25: 402-408, 2001.
45. Kaizuka T, Morishita H, Hama Y, Tsukamoto S, Matsui T, Toyota Y, Kodama A, Ishihara T, Mizushima T and Mizushima N: An autophagic flux probe that releases an internal control. Mol Cell 64: 835-849, 2016.
46. O'Prey J, Sakamaki J, Baudot AD, New M, Van Acker T, Tooze SA, Long JS and Ryan KM: Application of CRISPR/Cas9 to autophagy research. Methods Enzymol 588: 79-108, 2017.
47. Krypuy M, Newnham GM, Thomas DM, Conron M and Dobrovic A: High resolution melting analysis for the rapid and sensitive detection of mutations in clinical samples: KRAS codon 12 and 13 mutations in non-small cell lung cancer. BMC Cancer 6: 295, 2006.
48. Wilhelm SM, Carter C, Tang L, Wilkie D, McNabola A, Rong H, Chen C, Zhang X, Vincent P, McHugh M, *et al*: BAY 43-9006 exhibits broad spectrum oral antitumor activity and targets the RAF/MEK/ERK pathway and receptor tyrosine kinases involved in tumor progression and angiogenesis. Cancer Res 64: 7099-7109, 2004.
49. Chou TC: Theoretical basis, experimental design, and computerized simulation of synergism and antagonism in drug combination studies. Pharmacol Rev 58: 621-681, 2006.
50. Mukai S, Moriya S, Hiramoto M, Kazama H, Kokuba H, Che XF, Yokoyama T, Sakamoto S, Sugawara A, Sunazuka T, *et al*: Macrolides sensitize EGFR-TKI-induced non-apoptotic cell death via blocking autophagy flux in pancreatic cancer cell lines. Int J Oncol 48: 45-54, 2016.
51. Yoshii SR and Mizushima N: Monitoring and measuring autophagy. Int J Mol Sci 18: 2017.
52. Mauvezin C and Neufeld TP: Bafilomycin A1 disrupts autophagic flux by inhibiting both V-ATPase-dependent acidification and Ca-P60A/SERCA-dependent autophagosome-lysosome fusion. Autophagy 11: 1437-1438, 2015.
53. Moriya S, Komatsu S, Yamasaki K, Kawai Y, Kokuba H, Hirota A, Che XF, Inazu M, Gotoh A, Hiramoto M and Miyazawa K: Targeting the integrated networks of aggresome formation, proteasome, and autophagy potentiates ER stressmediated cell death in multiple myeloma cells. Int J Oncol 46: 474-486, 2015.
54. Miyahara K, Kazama H, Kokuba H, Komatsu S, Hirota A, Takemura J, Hirasawa K, Moriya S, Abe A, Hiramoto M, *et al*: Targeting bortezomib-induced aggresome formation using vinorelbine enhances the cytotoxic effect along with ER stress loading in breast cancer cell lines. Int J Oncol 49: 1848-1858, 2016.
55. Kazama H, Hiramoto M, Miyahara K, Takano N and Miyazawa K: Designing an effective drug combination for ER stress loading in cancer therapy using a real-time monitoring system. Biochem Biophys Res Commun 501: 286-292, 2018.
56. Brewer JW and Diehl JA: PERK mediates cell-cycle exit during the mammalian unfolded protein response. Proc Natl Acad Sci USA 97: 12625-12630, 2000.
57. Hamanaka RB, Bennett BS, Cullinan SB and Diehl JA: PERK and GCN2 contribute to eIF2alpha phosphorylation and cell cycle arrest after activation of the unfolded protein response pathway. Mol Biol Cell 16: 5493-5501, 2005.
58. Vincenz L, Jager R, O'Dwyer M and Samali A: Endoplasmic reticulum stress and the unfolded protein response: Targeting the Achilles heel of multiple myeloma. Mol Cancer Ther 12: 831-843, 2013.
59. Pluquet O, Pourtier A and Abbadie C: The unfolded protein response and cellular senescence. A review in the theme: Cellular mechanisms of endoplasmic reticulum stress signaling in health and disease. Am J Physiol Cell Physiol 308: C415-C425, 2015.
60. Nishida Y, Arakawa S, Fujitani K, Yamaguchi H, Mizuta T, Kanaseki T, Komatsu M, Otsu K, Tsujimoto Y and Shimizu S: Discovery of Atg5/Atg7-independent alternative macroautophagy. Nature 461: 654-658, 2009.

61. Yamaguchi H, Arakawa S, Kanaseki T, Miyatsuka T, Fujitani Y, Watada H, Tsujimoto Y and Shimizu S: Golgi membrane-associated degradation pathway in yeast and mammals. EMBO J 35: 1991-2007, 2016.
62. Chen C, Ju R, Shi J, Chen W, Sun F, Zhu L, Li J, Zhang D, Ye C and Guo L: Carboxyamidotriazole synergizes with sorafenib to combat non-small cell lung cancer through inhibition of NANOG and aggravation of apoptosis. J Pharmacol Exp Ther 362: 219-229, 2017.
63. Diaz R, Nguewa PA, Parrondo R, Perez-Stable C, Manrique I, Redrado M, Catena R, Collantes M, Peñuelas I, Díaz-González JA and Calvo A: Antitumor and antiangiogenic effect of the dual EGFR and HER-2 tyrosine kinase inhibitor lapatinib in a lung cancer model. BMC Cancer 10: 188, 2010.
64. Saddoughi SA, Gencer S, Peterson YK, Ward KE, Mukhopadhyay A, Oaks J, Bielawski J, Szulc ZM, Thomas RJ, Selvam SP, *et al*: Sphingosine analogue drug FTY720 targets I2PP2A/SET and mediates lung tumour suppression via activation of PP2A-RIPK1-dependent necroptosis. EMBO Mol Med 5: 105-121, 2013.
65. Heymach JV, Nilsson M, Blumenschein G, Papadimitrakopoulou V and Herbst R: Epidermal growth factor receptor inhibitors in development for the treatment of non-small cell lung cancer. Clin Cancer Res 12: 4441s-4445s, 2006.
66. McDermott MS, Browne BC, Conlon NT, O'Brien NA, Slamon DJ, Henry M, Meleady P, Clynes M, Dowling P, Crown J and O'Donovan N: PP2A inhibition overcomes acquired resistance to HER2 targeted therapy. Mol Cancer 13: 157, 2014.
67. Janne PA, Engelman JA and Johnson BE: Epidermal growth factor receptor mutations in non-small-cell lung cancer: Implications for treatment and tumor biology. J Clin Oncol 23: 3227-3234, 2005.
68. Gainor JF and Shaw AT: Emerging paradigms in the development of resistance to tyrosine kinase inhibitors in lung cancer. J Clin Oncol 31: 3987-3996, 2013.